Title
Functionally Assembled Terrestrial Ecosystem Simulator (FATES) for Hurricane Disturbance and Recovery

Journal
Journal of Advances in Modeling Earth Systems, 16(1)

ISSN
1942-2466

Authors
Shi, Mingjie
Keller, Michael
Bomfim, Barbara
et al.

Publication Date
2024

DOI
10.1029/2023ms003679

JAMES | Journal of Advances in Modeling Earth Systems

RESEARCH ARTICLE
10.1029/2023MS003679

Special section
Machine learning application to Earth system modeling

Functionally Assembled Terrestrial Ecosystem Simulator (FATES) for Hurricane Disturbance and Recovery

Mingjie Shi[1], Michael Keller[2,3], Barbara Bomfim[4], Lingcheng Li[1], Charlie Koven[4], Lara Kueppers[4,5], Ryan Knox[4], Jessica Needham[4], Shih-Chieh Kao[6], Peter E. Thornton[6], Michele M. Thornton[6], and L. Ruby Leung[1]

[1]Pacific Northwest National Laboratory, Richland, WA, USA, [2]USDA Forest Service, International Institute of Tropical Forestry, Pasadena, CA, USA, [3]Jet Propulsion Laboratory, Pasadena, CA, USA, [4]Lawrence Berkeley National Laboratory, Climate and Ecosystem Sciences, Berkeley, CA, USA, [5]University of California, Berkeley, CA, USA, [6]Oak Ridge National Laboratory, Oak Ridge, TN, USA

Abstract Tropical cyclones are an important cause of forest disturbance, and major storms caused severe structural damage and elevated tree mortality in coastal tropical forests. Model capabilities that can be used to understand post-hurricane forest recovery are still limited. We use a vegetation demography model, the Functionally Assembled Terrestrial Ecosystem Simulator, coupled with the Energy Exascale Earth System Model Land Model (ELM-FATES) to study the processes and the key factors regulating post-hurricane forest recovery. We implemented hurricane-induced forest damage, including defoliation, structural biomass reduction, and tree mortality, performed ensemble model simulations, and used random forest feature importance. For the simulation in the Luquillo Experimental Forest, Puerto Rico, we identified factors controlling the post-hurricane forest recovery, and quantified the sensitivity of key model parameters to the post-hurricane forest recovery. The results indicate a tendency for the Bisley forests to shift toward the light demanding plant functional type (PFT) when the pre-hurricane biomass between the light demanding and shade tolerant PFTs is nearly equal and forests experience hurricane disturbance with mortality >60% for both the two PFTs. Under more realistic conditions where the shade tolerant PFT is initially dominant, mortality >80% is required for a shift toward dominance of the light demanding PFT at Bisley. Hurricane mortality and background mortality are the two major factors regulating post-hurricane forest recovery in simulations. This research improves understanding of the ELM-FATES model behavior associated with hurricane disturbance and provides guidance for dynamic vegetation model development in representing hurricane induced forest damage with varied intensities.

Plain Language Summary To enhance the understanding of forest recovery after hurricanes, we implemented hurricane induced forest damage into the Functionally Assembled Terrestrial Ecosystem Simulator, coupled with the Energy Exascale Earth System Model Land Model (ELM-FATES). We performed ensemble ELM-FATES simulations with varied forest damage intensities in the Luquillo Experimental Forest, Puerto Rico, and used the output to identify factors controlling the post-hurricane forest recovery, which was further evaluated with random forest feature importance (RFFI) that quantifies the sensitivity of the key model parameters to the post-hurricane forest recovery. The results imply that hurricane mortality and background mortality are the major factors regulating post-hurricane forest recovery. Changes to the intensity of simulated hurricanes could alter forest composition and structure during recovery, which modifies forest ecological processes and potentially shift the wet forests in Puerto Rico to states with increased vulnerability to tropical cyclones. This research enhances our understanding of the ELM-FATES model behavior associated with hurricane disturbance and broadens the application of RFFI in quantifying the parameter sensitivity of a dynamic global vegetation model (DGVM). This research addresses the essential role of representing hurricane induced forest damage in DGVMs, an advanced tool for the future studies of tropical forest dynamics.

Key Points:

- Post-hurricane forest recovery favors the light demanding type when hurricane mortality rates are equal to or higher than 60% at Bisley
- Hurricane mortality and background mortality are the key factors regulating the post-hurricane forest recovery and biomass composition
- ELM-FATES simulations at a Puerto Rico forest site can represent reasonable GPP and ET seasonality but the flux magnitudes are biased low

Supporting Information:

Supporting Information may be found in the online version of this article.

Correspondence to:

M. Shi,
mingjie.shi@pnnl.gov

Citation:

Shi, M., Keller, M., Bomfim, B., Li, L., Koven, C., Kueppers, L., et al. (2024). Functionally assembled terrestrial ecosystem simulator (FATES) for hurricane disturbance and recovery. *Journal of Advances in Modeling Earth Systems*, *16*, e2023MS003679. https://doi.org/10.1029/2023MS003679

Received 16 FEB 2023
Accepted 17 NOV 2023

Author Contributions:

Conceptualization: Mingjie Shi, Michael Keller

1. Introduction

Tropical cyclones are a dominant form of disturbance in coastal tropical and sub-tropical forests. In the past 30 years, Puerto Rico experienced five cyclonic storms (hereafter *hurricanes*) greater than category 3 (i.e., wind speed greater than 178 km hr^{-1}); these major storms caused intense forest mortality and severe forest structural damage (Uriarte et al., 2019). Hurricane disturbance can affect biodiversity, species interactions, the

Data curation: Mingjie Shi, Barbara Bomfim, Shih-Chieh Kao, Peter E. Thornton, Michele M. Thornton
Formal analysis: Mingjie Shi
Funding acquisition: L. Ruby Leung
Investigation: Mingjie Shi, Barbara Bomfim
Methodology: Mingjie Shi, Michael Keller, Charlie Koven, Lara Kueppers, Ryan Knox, Jessica Needham
Project Administration: L. Ruby Leung
Resources: L. Ruby Leung
Software: Mingjie Shi, Lingcheng Li
Supervision: L. Ruby Leung
Validation: Mingjie Shi
Visualization: Mingjie Shi
Writing – original draft: Mingjie Shi
Writing – review & editing: Mingjie Shi, Michael Keller, Charlie Koven, Lara Kueppers, Ryan Knox, Jessica Needham, L. Ruby Leung

spatiotemporal dynamics of populations and communities, and biogeochemical cycling (Brokaw et al., 2012; Chazdon, 2003; Walker, 2012; Zimmerman et al., 2021). Hurricane disturbance can have tremendous and spatially heterogeneous impacts on tropical forests, but their representation in Earth System Models (ESMs) is limited. To build a foundation for representation of hurricane damage and post-hurricane recovery on tropical forest, we studied Hurricane Hugo (18 September 1989), a category 4 hurricane that passed the Luquillo Experimental Forest (LEF), located in northwestern Puerto Rico (Walker et al., 1992), a site of long-term ecological studies. Hugo defoliated the entire forest area while causing severe structural damage that varied spatially. Explicitly, Hugo reduced the aboveground biomass by 50% in the windward Bisley Experimental Watersheds (hereafter Bisley) (18°20' N, 65°50' W) in the east area of LEF, while biomass reduction in the leeward El Verde study site (18° 19' N, 65° 49' W), was minimal (Drew et al., 2009).

ESMs are limited by spatial resolution and the representation of vegetation. Specifically, most ESMs are run at spatial resolutions of 1–2° or coarser (Eyring et al., 2016). Vegetation dynamics are not sufficiently represented in ESMs. For example, Dirmeyer et al. (2021) used the simulation output from 37 models from the Climate Model Intercomparison Project Phase 6 (CMIP6) to study the impacts of carbon dioxide variation on hydroclimate, but only nine out of the 37 models include dynamic vegetation modules. Among these models that can represent vegetation dynamics, only a few models have wind disturbance processes included. By implementing typhoon-induced biomass reduction into the Spatial Explicit Individual-Based Dynamic Global Vegetation Model (SEIB-DGVM), Wu et al. (2019) simulated the impacts of typhoon on the carbon dynamics of a cool-temperate forest in northern Japan. ORCHIDEE-CAN is the only land surface component that can capture the dynamics of forest structure due to storm disturbance on both regional and global scales (Chen et al., 2018). The Ecosystem Demography model version 2 (ED2) can be employed as a dynamic global vegetation model (DGVM), and the first simulations using an offline version of the ED2 for studies of hurricane damage and forest recovery were performed at the El Verde site in Puerto Rico (Feng et al., 2017). Similarly, Zhang, Bra, et al. (2022) and Zhang, Heartsill-Scalley, and Bras (2022) implemented a hurricane induced wind mortality module and a seedling recovery module into ED2 and projected the recovery trajectory of plant function type (PFT) composition, size structure, and stem density, at the Bisley site in Puerto Rico. Using the Functionally Assembled Terrestrial Ecosystem Simulator (FATES), which has been coupled with the Energy Exascale Earth System Model (E3SM) Land Model (ELM-FATES), Negron-Juárez et al. (2020) implemented some simplified processes such as clear-cut and windthrow to represent forest disturbance. A selective logging module that can specify the timing and aerial extent of logging events and represent ecological, biophysical, and biogeochemical processes following a logging event has been implemented into ELM-FATES (Huang et al., 2020). Here, processes associated with hurricane disturbance and recovery are still under development in most of the DGVMs.

In this study, we aim to advance the understanding of the key plant-physiology-related parameters that regulate the post-hurricane forest recovery and enhance the ability of ELM-FATES to represent hurricane disturbance and post-hurricane recovery of tropical forests. We first use ELM-FATES to quantitatively estimate post-hurricane forest recovery rates and forest compositional changes. We perform numerical experiments to study the effects of hurricane damage on forest structure, with hurricane damage represented by defoliation, structural biomass reduction, and mortality in the model. We then examine how hurricanes with varied disturbance intensities affect the forest recovery rates and forest composition in terms of the biomass among different PFTs. Based on ELM-FATES ensemble simulations, this study also uses the Random Forests method (Breiman, 2021) to identify essential parameters that regulate the post-hurricane forest biomass recovery. We aim to improve understanding of the sensitivity of modeled forest recovery rates and composition to (a) pre-hurricane forest composition, (b) hurricane disturbance with varied intensity, and (c) the key model parameters that characterize the selected PFTs. Lastly, to evaluate how well ELM-FATES represents the photosynthetic carbon assimilation and land–atmosphere water exchange, we perform model-data comparison by taking the ensemble mean of the simulations with realistic forest status and using multiple data sets. This research lays the foundation for using ELM-FATES to understand post-hurricane vegetation dynamics.

2. Methods

2.1. Research Site and the Observational Data

We focused our numerical experiments on the Bisley Experimental Watersheds located in the east part of LEF, in northeastern Puerto Rico. The mean monthly temperature is 23.5–27°C and mean annual rainfall is 3,208 mm

(Brown et al., 1983; Garcia-Martino et al., 1996). As suggested by the annual precipitation amount at Bisley and the research by Running et al. (2004), the study site, similar to much tropical forest, is radiation limited in terms of vegetation productivity development. Thus, hurricane-induced water stress relief is not a factor evaluated in this study. Tabonuco forest, named after a prominent species at Bisley (*Dacryodes excelsa*.; Common name tabonuco), occupies the greatest area of LEF, and usually has trees mixed with lianas and canopies ranging from 25 to 30 m in height (Heartsill-Scalley, 2017) when mature. The forests in LEF have been affected by varying intensities and scales of disturbances, including hurricanes. The LEF has been impacted by the major hurricanes Hugo in 1989, Georges in 1998, and Irma and Maria in 2017. Hurricane Hugo, which made landfall at Puerto Rico on 18 September 1989, defoliated the entire area and reduced the aboveground biomass by 50% at Bisley (Drew et al., 2009).

In 1989, 86 permanent forest plots with a cumulative area of 0.71 ha were established in Bisley (Heartsill-Scalley et al., 2010). Measurements at all plots are taken at a 5-year interval; all stems ≥2.5 cm diameter at 1.3 m from the ground (i.e., DBH) are measured at the site. In this study, we use the Bisley tree census data from the US Forest Service Research Data Archive (Zhang, Bra, et al., 2022; Zhang, Heartsill-Scalley, & Bras, 2022) to calculate the hurricane mortality rates of each PFT based on censuses conducted 3 months before and 3 months after hurricane Hugo (18 September 1989) (Heartsill-Scalley et al., 2010; Zhang, Bra, et al., 2022; Zhang, Heartsill-Scalley, & Bras, 2022). In the post-Hugo survey, trees were considered dead if there was no evidence of resprouting along the branches or stems, no leaves, no new leaves, more than 50% root exposure, stem breakage, or no tree in place of where there once was a tree. We assign censused trees to two PFTs, light demanding and shade tolerant, based on traits compiled by Adame et al. (2014) (Section 2.3). We estimate the mortality from hurricane Hugo as the ratio of the number of stems that existed in the pre-Hugo census but not in the post-Hugo census to the number of stems that existed in the pre-Hugo census (Zhang, Bra, et al., 2022; Zhang, Heartsill-Scalley, & Bras, 2022) and find that the hurricane mortality rate for the light demanding PFT was 52% while that of the shade tolerant PFT was 45%.

We also use the measurements at Bisley to evaluate the model performance before Hurricane Hugo. The biomass sampling at Bisley in September 1989, provides above-ground biomass (AGB) information for all species before Hurricane Hugo (Scatena et al., 1996). The relative contribution of each PFT to the overall forest biomass is used to evaluate pre-hurricane forest biomass partitioning among the light demanding and shade tolerant PFTs simulated by ELM-FATES. The observations suggested the biomass partition between the light demanding and shade tolerant PFTs is 29% versus 71%, and this biomass partition is used to evaluate the ELM-FATES spin-up, which is discussed in Section 2.4.2.

2.2. ELM-FATES

We use ELM-FATES (Fisher et al., 2015; Holm et al., 2020; Koven et al., 2020) to study the post-hurricane forest recovery at the Bisley site. ELM is based on the Community Land Model Version 4.5 (CLM4.5) with new options for representing soil hydrology and biogeochemistry (Burrows et al., 2020). ELM-FATES is developed with the Ecosystem Demography (ED) concept of a cohort-based representation of vegetation dynamics (Moorcroft et al., 2001). Different from the *big-leaf* structure, ED and FATES separate the landscape into implicit *patches* according to age since last disturbance. The landscape-scale age distribution resulting from disturbance is represented with a patch fusion/fission scheme, which tracks the landscape-scale age. In different patches, individual plants are grouped into cohorts by PFTs and height classes. This grouping method captures the dynamic matrix of disturbance recovery processes in a forest ecosystem. Thus, ELM-FATES tracks the changing abundance of trees of different sizes and PFTs arising from tree growth, mortality, recruitment, and the impact of disturbances. Similar to the original ED formulation, ELM-FATES bases growth and allocation on observed plant allometric relationships, yet diverges in its representation of the light environment by using the perfect plasticity approximation (PPA) that describes the crown spatial arrangements throughout the canopy and organizes cohorts into discrete canopy layers (Fisher et al., 2010; Purves et al., 2008). Plant mortality is attributed to background mortality (i.e., the mortality observed in a stand in the absence of abrupt disturbances; Taccoen et al., 2019), carbon starvation, hydraulic failure, freezing stress, and optionally size dependent senescence, all of which reflect plant responses to environmental factors and to ecosystem structure.

2.3. ELM-FATES Parameterization

To obtain reasonable ELM-FATES simulations at Bisley, we perform model parameterization. By following the field data grouping method (Section 2.1), all the ELM-FATES simulations are performed by using two PFTs:

Table 1
Parameterization of the Light Demanding and Shade Tolerant PFTs at Bisley

Parameter names	Units	Light demanding	Shade tolerant	Reported ranges	Reference for the parameter value range
Specific leaf area	$m^2\ gC^{-1}$	0.015	0.014	0.01–0.017	Feng et al. (2017) [a]
Vcmax at 25°C	umol $m^{-2}s^{-1}$	65	45 (47.5[b])	20.0–75.0	Kattge et al. (2009)
Specific wood density	g cm^{-3}	0.4	0.65 (0.625[b])	0.5–0.8	Reyes et al. (1992) [a]
Leaf longevity	yr	0.9	2.6	0.8	Kattge et al. (2011)
Background mortality rate	yr^{-1}	0.047	0.02	0.02–0.05	Powell et al. (2018)
Leaf N:C	gN gC^{-1}	0.043	0.025	0.043	Kattge et al. (2011)
Root longevity	yr	0.9	2.6	1.17–16.7	Feng et al. (2017) [a]
Fine root N:C	gN gC^{-1}	0.035	0.035	0.036	Silver and Miya (2001)
Allocation of fine root C per leaf C	gC gC^{-1}	0.62	0.62	0.56–2.37	Feng et al. (2017) [a]
Growth respiration factor	unitless	0.3	0.3	0.19–0.61	Feng et al. (2017) [a]
Fraction of plants in understory cohort impacted by overstorey treefall (ecosystem-level)	unitless	0.625	0.625	0–1	Koven et al. (2020)

Note. Parameter values are based on cited studies of the pantropics.
[b]The adjusted parameter values for SPINUP2, which is introduced in Section 3.1. [a]The parameter values in the paper are specifically obtained from Puerto Rico.

light demanding and shade tolerant broadleaf tropical evergreens. We first use a tropical forest parameter set that minimizes bias against observed basal area, leaf area, growth increment and mortality rate at Barro Colorado Island Panama (BCI), a tropical forest site, as drawn from an ensemble of perturbed parameter simulations (Koven et al., 2020). We then refer to Huang et al. (2020) to parameterize these two PFTs. These parameter values permit co-existence of two PFTs and are consistent to observed values across the pantropical range (e.g., Kattge et al., 2009; Powell et al., 2018). We focus on the adjustment of parameters that distinguish plant functional strategies and these parameters include top-of-canopy values for maximum carboxylation at reference temperature ($Vcmax_{25,top}$), leaf N:C, leaf longevity, among others (Table 1). We reduce the $Vcmax_{25,top}$ value of the shade tolerance PFT from 50 μmol $m^{-2}\ s^{-1}$, which is suggested by Huang et al. (2020), to 45 μmol $m^{-2}\ s^{-1}$ in order to better fit in the leaf economic spectrum (i.e., the relationships between $Vcmax_{25,\ top}$, specific leaf area, and area-based value of leaf nitrogen; Walker et al., 2014). Wood density follows observations in tropical America (Reyes et al., 1992) as shown for the shade tolerant PFT are included in Table S1 in Supporting Information S1. We perform model simulations by following the parameterization discussed above (Sections 2.4.2 and 3.1). To better match the observations, we also adjust the parameter values of $Vcmax_{25,top}$ and specific wood density of the shade tolerant PFT to favor a faster growth of the shade tolerant PFT. Specifically, we increase the value of $Vcmax_{25,top}$ from 45 to 47.5 μmol $m^{-2}\ s^{-1}$, and reduce the specific wood density value from 0.65 to 0.625 g cm^{-3}. The parameter values of the light demanding PFT are not changed. This update maintains the parameter values in reasonable ranges (Table 1) and reproduces PFT-based AGB partitions more consistent with observations (Section 3.1). We include the parameter values in Table 1 and more details of ELM-FATES parameterization of this study are discussed in Text S1 in Supporting Information S1.

2.4. Model Configuration and Experimental Design

The overall design for our numerical experiments is illustrated in Table 2. We conduct experiments with two spin-up conditions that represent different distributions of the PFTs. With PFTs nearly evenly divided, we conduct Experiments A to understand how rates of hurricane mortality affect the relative recovery of each PFT. Using the more realistic PFT distribution, we repeat the manipulation of mortality rates (Experiment B). Thereafter, we adjust mortality rates to reflect those measured in the field by repeated inventories (Experiment C). In a final set of experiments, we test parameter sensitivities (Experiment D). Using the ensemble of the model runs we then compared the simulations to data representing ecosystem fluxes (Experiment E). In all the simulations, ambient CO_2 concentration is fixed, with the value of 367 ppm; in other words, the impacts of CO_2 fertilization on forest recovery rates are not considered in this study.

Table 2
The Experimental Design of This Study

Experiment name	The initial condition	$R_{biomass\_LD:TOT}$: $R_{biomass\_ST:TOT}$	Experimental design	Description
A	SPINUP1	48%: 52%	Even hurricane mortality values for LD and ST	Section 3.2.1 & Table S2 in Supporting Information S1
B	SPINUP2	29%: 71%	Even hurricane mortality values for LD and ST	Section 3.2.1 & Table S3 in Supporting Information S1
C	SPINUP2	29%: 71%	Realistic hurricane mortality rates	Section 3.2.2 & Table S4 in Supporting Information S1
D	SPINUP2	29%: 71%	Parameter sensitivity tests and random forest feature importance estimates	Section 3.3 & Table S5 in Supporting Information S1
E	SPINUP2	29%: 71%	Model–data comparison by using the model ensemble simulations with observed hurricane mortality rates	Section 3.4

Note. LD represents the light demanding PFT and ST represents the shade tolerant PFT. $R_{biomass\_LD:TOT}$ indicates the ratio between the light demanding biomass to the total biomass, and $R_{biomass\_ST:TOT}$ indicates the ratio between the shade tolerant biomass to the total biomass. The details of each sub-experiment are referred to Tables S2–S6 in Supporting Information S1.

2.4.1. Model Driving Data

We use the meteorological forcing data from Daymet, which provides gridded estimates of daily weather parameters at the 1 km spatial resolution from 1950 to present for Puerto Rico (Thornton et al., 2021; Figure S1 in Supporting Information S1). Using the sub-daily temporal information from other meteorological reanalysis data sets, Daymet was further temporally downscaled to 3-hourly time steps and provided in the format required for ELM simulations (Kao et al., 2022). The process of temporal downscaling preserved the relative magnitude in each sub-daily time step while maintaining the total and average Daymet values on each day. The widely used Global Soil Wetness Project Version 3 (GSWP3; Yoshimura & Kanamitsu, 2013) meteorological reanalysis data set for offline land surface model simulation and diagnosis was selected to temporally downscale Daymet from 1950 to 2014. Since GSWP3 is not available after 2014. We used NCEP North American Regional Reanalysis (NARR; Mesinger et al., 2006) to extend the temporal downscaling of Daymet to 2017. We also compared the overlapping 1980–2014 sub-daily Daymet downscaled by GSWP3 and NARR to verify that the change from GSWP3 to NARR does not cause biases. Here, we cycle the sub-daily Daymet forcing during 1950–1959 30 times to spin-up the model for 300 years (Koven et al., 2020). Beginning from the spun-up case, we perform hurricane disturbance simulations during 1950–2017.

2.4.2. Model Spin-Ups

To understand how pre-hurricane forest composition affects post-hurricane forest recovery characteristics, we perform two spin-up simulations, one with a nearly even biomass partition between the light demanding and shade tolerant PFTs (SPINUP1) and the other spin-up with biomass partition that reflects the observational data (SPINUP2; Section 2.1). The difference between the two spin-up conditions depends on parameter values for $Vcmax_{25,top}$ and specific wood density (Table 1). We perform model simulations by using the model initial files from these two spin-ups (Table 2). The purpose of performing simulations with SPINUP1 is to study if the model can return to the pre-perturbation status or shift the PFT distributions with an even pre-hurricane biomass partition between PFTs and hurricane disturbance at varied intensity. We also adjust parameter values for SPINUP2 to obtain a more realistic biomass partition that is suggested by observations (Table 1). The spin-up results are discussed in Section 3.1.

2.4.3. Implementation of Hurricane Disturbance

We implement hurricane disturbance with different intensities through processes of defoliation, 20% sapwood and structural organ biomass reduction (herein structural damage) to the surviving trees, and hurricane-induced mortality rates. Defoliation is imposed on ELM-FATES by prescribing the timing of leaf-off and leaf-on in the phenology module. The loss of biomass from trees surviving the hurricane is imposed in ELM-FATES by briefly increasing the sapwood and structure turnover rates. The default turnover rate (i.e., turnover time frames) of these two components is 150 years. We assume that hurricane disturbance raises this turnover rate to 0.014 years (i.e., 5 days). This increased turnover rate is applied to the model for one model day leading to an integrated loss of

~20% of the woody biomass. To further represent hurricane-induced forest damage, we add a hurricane mortality term in the model, which can be prescribed to represent different hurricane mortality rates for the two PFTs. This hurricane mortality term will only be applied to the model for one day when a hurricane happens, and it will be added to the total mortality rate, which consists of background mortality, carbon starvation mortality, hydraulic failure mortality, freezing stress mortality, and optionally size dependent senescence. Based on the model structure of ELM-FATES, these three disturbance types will be applied to the model in the order of (a) defoliation, (b) hurricane induced mortality, and (c) structural damage. Thus, the structural damage will be only applied to surviving trees. In terms of the disturbance intensity, we applied all three types of damage to the Bisley forests. These damage types can be independently applied in ELM-FATES to represent hurricane disturbance with various intensity.

2.4.4. ELM-FATES Simulated Biomass Recovery Sensitivity to Hurricane Mortality Rates

Hurricane disturbance intensity is determined by the features of a hurricane (e.g., wind speed, pathways) and the pre-hurricane forest status (e.g., species composition, age, and soil moisture; Uriarte et al., 2019); as a result, it varies much with specific hurricane events. In other words, it's difficult to estimate the mortality rate difference between PFTs, so we perform both hypothetical (Section 2.4.4) and quasi-realistic (Section 2.4.5) simulations in this study. We first perform model simulations by assuming both the light demanding and shade tolerant PFTs experience the same hurricane-induced mortality rates, which range from 30% to 90% (Table S2 and Figure S3 in Supporting Information S1), to evaluate the post-hurricane forest biomass recovery from varied hurricane mortality rates. These simulations are combined with other disturbance types, including mortality-only, defoliation and mortality, and defoliation, structural damage and mortality as shown in the three simulations groups of Table S2 in Supporting Information S1. For all the simulations with hurricane mortality, we assume only one major hurricane disturbed Bisley during 1950–2017. We simulate all types of disturbance on 1 September 1950, and run the model for 1950–2017 after the model spin-up. Simulations with this time frame allow for an understanding of the long-term (~70 years) post-hurricane forest behavior. We use the ELM-FATES initial files from both SPINUP1 and SPINUP2 for Experiment A and Experiment B, respectively (Table 2). The experimental design is hypothetical and used to study the competition between the two PFTs when they are equally and realistically disturbed.

2.4.5. Observation-Driven Hurricane Simulations

Besides performing hypothetical simulations that are discussed in Section 2.4.4 (Table S2 in Supporting Information S1), we also consider three alternate scenarios of hurricane-driven mortality informed by observations and literature. Using observed differences in hurricane mortality rates among species at Bisley, we estimate that the hurricane mortality rates of the light demanding and shade tolerant PFTs are 52% and 45%, respectively (Section 2.1). The simulation with this mortality distribution between PFTs is named hurricane disturbance C1 (Tables 2 and Table S4 in Supporting Information S1). We also use hurricane-induced mortality rates suggested by Zhang, Bra, et al. (2022) and Zhang, Heartsill-Scalley, and Bras (2022), which summarized the hurricane mortality rate variations among PFTs during Hurricane Hugo, 1989 and Hurricane Maria, 2017. According to Zhang, Bra, et al. (2022) and Zhang, Heartsill-Scalley, and Bras (2022), the Hugo induced mortality rate of the light demanding trees is ~80%. Because the PFT partition in our study does not include the mid-successional and palm PFTs included by Zhang, Bra, et al. (2022) and Zhang, Heartsill-Scalley, and Bras (2022) and we use the species-to-PFT grouping method from Adame et al. (2014), we assign 50% mortality for the shade tolerant PFT (Zhang, Bra, et al., 2022; Zhang, Heartsill-Scalley, & Bras, 2022). This simulation is named hurricane disturbance C2 (Tables 2 and Table S4 in Supporting Information S1). To understand the sensitivity of forest recovery to different hurricane mortality rate combinations, we also applied another group of mortality values with 50% and 35% for the light demanding and shade tolerant PFTs, respectively (Figure S2 in Supporting Information S1), by referring to the summarized forest mortality values for hurricane Maria (Zhang, Bra, et al., 2022; Zhang, Heartsill-Scalley, & Bras, 2022). This simulation is named hurricane disturbance C3 (Tables 2 and Table S4 in Supporting Information S1). All these simulations use the restart file from SPINUP2, with biomass partitions between the two PFTs constrained by observations.

2.4.6. Forest Recovery Rates

One of the research goals is to study the forest recovery rate variations due to hurricane disturbance with different intensity. Thus, we estimate the forest recovery rates (herein $R_{recovery}$; kgC m^{-2} yr^{-1}) by calculating the linear regression coefficient of the biomass in the first 10 simulation years after the hurricane disturbance (i.e.,

1951–1960). The regression coefficient values for the two PFTs are shown in Figure 3, in which we use the simulation results with defoliation and structural damage (herein D-$SB_{reduction}$) as well as different hurricane mortality rates implemented (Experiments A3 and B3; Tables S2 and S3 in Supporting Information S1). To further understand the use of ELM-FATES output during 1951–1960 for the calculation of $R_{recovery}$, we also test $R_{recovery}$ variations with different recovery time frames. We calculate $R_{recovery}$ by using the model output based on initial files of both SPINUP1 and SPINUP2 during the time frames of 1951–1955, 1961–1970, and 1951–1970 (Figures S4 and S5 in Supporting Information S1).

2.5. Parameter Sensitivity Tests and Importance Quantification

We explore the parameter sensitivity for the light demanding and shade tolerant PFTs in simulated post-hurricane forest recovery. With ELM-FATES, we perturb seven parameters (the first seven rows in Table 1) used to characterize these two PFTs (Huang et al., 2020). Each parameter that has two values to separate these two PFTs is perturbed by up to 10%. We use the Latin Hypercube method for the parameter perturbation. If the perturbations induce unrealistic parameter value distributions, such as lower versus higher $Vcmax_{25,top}$ values between the light demanding and shade tolerant PFTs, we instead use the perturbation-suggested parameter values for the light demanding PFT, and then calculate the perturbed parameter value of the shade tolerant PFT by using a fixed difference in parameter values between the two PFTs (Table 1). With this method, we obtain 350 ensemble members for the hurricane disturbance simulations. We also apply different hurricane mortality rate combinations between the light demanding and shade tolerant PFTs to the parameter sensitivity tests. This way, the mortality rates of the two PFTs can be quantified as another factor regulating the post-hurricane forest recovery. As discussed in Section 3.2.1, the hurricane mortality rate of 60% is crucial to both PFTs in terms of the forest recovery rates and recovery status for a forest with a nearly equal biomass partition for the two PFTs. Thus, we also implement the mortality rates of 60% for both PFTs for the model ensemble simulations. We also use the mortality values of 52% and 45% for the light demanding and shade tolerant PFTs, respectively, to better match the observed mortality rates (Section 2.4.5). To consider reasonable uncertainty ranges of the mortality values, we additionally use four groups of mortality values for the light demanding and shade tolerant PFTs as: 80% and 50%, 50% and 80%, 50% and 35%, and 35% and 50%, respectively. With 350 parameter ensemble members of each hurricane mortality rate combination, simulations are performed 6 times by using the six mortality rate groups (Table S5 in Supporting Information S1). Thus, we have a total of 2100 ensemble members, which can be used to quantify the feature importance of the seven parameters and the hurricane mortality rates. Parameter sensitivity tests are performed by using the spun-up results of SPINUP2, which tends to be more consistent with the observed pre-Hugo biomass composition. These simulations include D-$SB_{reduction}$.

We explore parameter sensitivity under post-hurricane forest recovery conditions with the Random Forests algorithm. Random Forests (RF) is an ensemble learning method consisting of a set of decision trees (Breiman, 2021). RF has been widely applied in the earth and environmental science field (Belgiu & Drăguţ, 2016; Jung et al., 2020; Thessen, 2016; Tyralis et al., 2019), including parameter sensitivity analysis (Antoniadis et al., 2021; Huang & Boutros, 2016). RF based sensitivity analysis has many advantages including its effectiveness and easy application, its ability to implicitly deal with correlation and high dimensional data, and handle interactions between variables (Antoniadis et al., 2021).

We train RF surrogate models to emulate the ELM-FATES model behavior and analyze the parameter importance by using all the ELM-FATES based ensemble simulations (Hao et al., 2021). As discussed above, 16 variables are used as the RF model features, including 14 parameters in Table 1 and two hurricane mortality rates for the two PFTs. The ELM-FATES outputs, including both $R_{recovery}$ and the PFT-level annual mean biomass across 2008–2017 are used as the RF model targets. Specifically, we calculate $R_{recovery}$ by using the biomass values during 1951–1960 and use the RF feature importance to quantify the contributions of the parameters and hurricane mortality rates to $R_{recovery}$ in the first 10 recovery years after the hurricane disturbance. We particularly compare $R_{recovery}$ between the light demanding and shade tolerant PFTs and quantify the parameter importance related to whether the light demanding $R_{recovery}$ is larger or smaller than the shade tolerant $R_{recovery}$, represented as $R_{LD} \geq R_{ST}$ and $R_{LD} < R_{ST}$, respectively, where R_{LD} represents the $R_{recovery}$ of the light demanding PFT and R_{ST} represents the $R_{recovery}$ of the shade tolerant PFT. To evaluate the forest biomass recovery status during 2008–2017, we quantify the biomass ratio of each PFT change. In other words, if the biomass ratio between the light demanding biomass to total biomass is larger than 29%, the light demanding biomass ratio before the hurricane disturbance,

we define this status as light demanding biomass ratio increase, and vice versa. The same biomass quantification method is also applied to the shade tolerant PFT by using the biomass ratio of 71%. The feature importance derived from the RF surrogate model measures how important a feature (e.g., parameter) is for predictive performance of the model, which can be used as a proxy to quantify parameter sensitivity.

2.6. Observational Data Used for ELM-FATES Evaluation

Due to the lack of in situ carbon and water flux measurements at Bisley, we use multiple gross primary production (GPP) and evapotranspiration (ET) estimates to evaluate the GPP and ET simulations of ELM-FATES. The GPP products include (a) FluxCom GPP (Jung et al., 2020), (b) the GPP based on the moderate-resolution imaging spectroradiometer (MODIS; Zhao et al., 2005), and (c) the Orbiting Carbon Observatory-2 (OCO-2) Solar-induced chlorophyll fluorescence (SIF) derived GPP (Li & Xiao, 2019). We also use the ET product obtained from the MODIS measurements (Mu et al., 2011) and an ET product based on the MODIS measurements and Modern-Era Retrospective analysis for Research and Applications, version 2 (MERRA-2), utilizing the ET algorithm of Priestley Taylor-Jet Propulsion Laboratory (PT-JPL; Purdy et al., 2018). Furthermore, we process the latent heat flux (J m^{-2} day^{-1}) from FluxCom (Jung et al., 2020) to obtain another ET product. These data sets have different spatial and temporal resolutions, and the detailed information is summarized in Table S6 in Supporting Information S1. All these data sets are gridded globally, and the values in the grid cells co-located with Bisley are selected for the model-data comparison. We use the monthly records of each data product and estimate the GPP and ET seasonality based on the multi-year mean. Because of the data variability (Section 3.4), we also calculate the arithmetic mean of different data sources.

3. Results

3.1. Model Spin-Up

As discussed in Section 2.4.2, we run the model for 300 years of spin-up (Table 2). SPINUP1 uses parameter values listed in Table 1. Under this parameterization, the biomass-to-total biomass ratios of the light demanding and shade tolerant PFTs are ∼48% and ∼52%. Compared to pre-Hugo field census, which suggests 29% and 71% of the AGB from the light demanding and shade tolerant PFTs, respectively (Section 2.1), SPINUP1 represents a hypothetical forest with almost equal abundance of shade tolerant and light demanding PFTs. Maintaining these two parameters within reasonable ranges, SPINUP2 (Sections 2.3 and 2.4.2) partitions biomass more consistently with observational data, 27% and 73% of the AGB from the light demanding and shade tolerant PFTs, respectively.

3.2. Hurricane Disturbance Simulations

3.2.1. Hypothetical Hurricane Disturbance Simulations With ELM-FATES

To study the forest recovery associated with hurricane disturbance with different intensities, we implement hurricane disturbance in ELM-FATES. We first use the spun-up result from SPINUP1 to initialize a simulation case and perform the defoliation-only simulation, in which defoliation happens on 1 September 1950. We assume that the hurricane induces an 100% defoliation. Based on the defoliation-only code, we then implement the representation of structural biomass reduction in the model. We name the simulations with both defoliation and structural biomass reduction as D-$SB_{reduction}$ (Figure 1). By comparing the monthly output in September and October of 1950, the defoliation-only simulation instantaneously induces 1.2% of total biomass reduction for both the light demanding and shade tolerant PFTs. Implementing the sapwood and structural organ biomass reduction (∼20%) results in more total biomass reduction at rates of 13.9% and 15.0% for the light demanding and shade tolerant PFTs, respectively.

We further compare forest succession between the disturbed simulations and the simulation without any hurricane induced forest disturbance, and calculate the total biomass of the light demanding and shade tolerant PFTs in the last 10 simulation years (2008–2017). During 2008–2017, the defoliation-only simulation (Figures not shown) induces 0.5% and −0.1% of total biomass change of light demanding and shade tolerant PFTs, respectively, while the simulation of D-$SB_{reduction}$ results in 1.3% and 1.1% of total biomass reductions of the same two PFTs, respectively (Figure 1). The defoliation-only simulation causes a minimal AGB change right after the hurricane

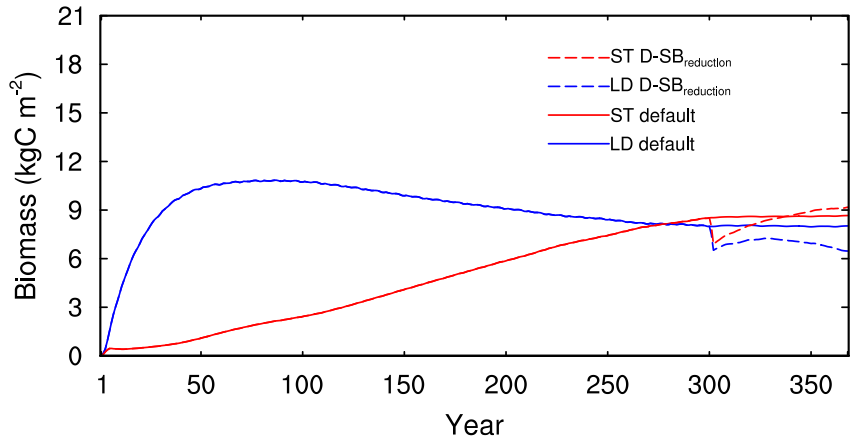

Figure 1. The forest development trajectories of light demanding and shade tolerant PFTs for the simulation without any hurricane induced forest disturbance (herein default; solid-line) and simulation with defoliation and structural biomass reduction (i.e., D-$SB_{reduction}$; dashed-line) at Bisley. LD represents the light demanding PFT and ST represents the shade tolerant PFT.

disturbance (in September 1950), and the forest recovers toward the end of the model simulation period. Therefore, we do not further analyze the defoliation-only simulation.

In the mortality sensitivity analysis, we analyze the simulation trajectories and calculate the mean total biomass of the two PFTs in the last 10 simulation years for the comparison between different simulation groups. In the mortality-only (Experiment A1) and defoliation and morality (Experiment A2) simulations, the light demanding PFT is favored with relatively larger biomass values among the simulation sub-groups with hurricane mortality rates of 75% or larger (Table S2 in Supporting Information S1). Experiment A3 has both D-$SB_{reduction}$ and hurricane mortality rates implemented, and we find that the biomass divergence between the shade tolerant and the light demanding PFTs is the largest when the hurricane mortality rates are 75%, 80%, and 90% (Figure 2c). Compared to experiments of A1 and A2, when the mortality rates are 60% or larger, Experiment A3 results in the least biomass of the shade tolerant PFT among Experiments A1–A3 (Figure 2b) and the biomass of the light demanding PFT tends to increase with the increase in mortality rates among all the three experiment groups (Table S2 in Supporting Information S1 and Figure 2a). In Experiment A3, the biomass of the light demanding PFT is more than that of the shade tolerant PFT for a difference of 0.77 kgC m^{-2} between the two PFTs when the hurricane mortality rate is 70% (Table S2 in Supporting Information S1 and Figure 2c). In the simulations without structural biomass reduction (i.e., A1 and A2), the hurricane mortality rates need to be 75% or larger for the biomass of the light demanding PFT to be higher than that of the shade tolerant PFT (Table S2 in Supporting Information S1 and Figure 2c). When the mortality rates are 60%–70%, the biomass difference between the two PFTs diverge more than that estimated by experiments with other mortality rates among the three simulation groups (Figure 2c). Within this mortality range, implementing defoliation as well as structural biomass reduction favors the biomass recovery of the light demanding PFT (Figures 2a and 2c). Thus, the experiments with different disturbance scenarios suggest a critical range of mortality values between 60% and 70% in determining the post-hurricane biomass recovery and the divergence of PFT-level biomass characterized by hurricane disturbance of different types (e.g., defoliation, structural biomass reduction).

Similar conclusions can also be obtained from Figure S3 in Supporting Information S1, which is based on Experiment A3. The total biomass trajectories between the two PFTs suggest that model simulated biomass partitions between PFTs tend to return to the pre-perturbation status when only defoliation and structural biomass reduction are implemented in the model (Figure S3 and Table S2 in Supporting Information S1). When the hurricane mortality values are 70% and larger for both of the two PFTs, the forests start shifting PFT distributions (Figures S3e–S3i in Supporting Information S1). The total biomass trajectories between the two PFTs suggest that the light demanding PFT is favored most with the hurricane mortality rate of 90% (Figure S3i in Supporting Information S1). In other words, ELM-FATES suggests that with severe hurricane disturbances, the forests tend to recover to an ecosystem dominated by the light-demanding trees. When the mortality values are 75% or larger, the biomass difference between the different tests starts to decrease. This result indicates that in forests with severe

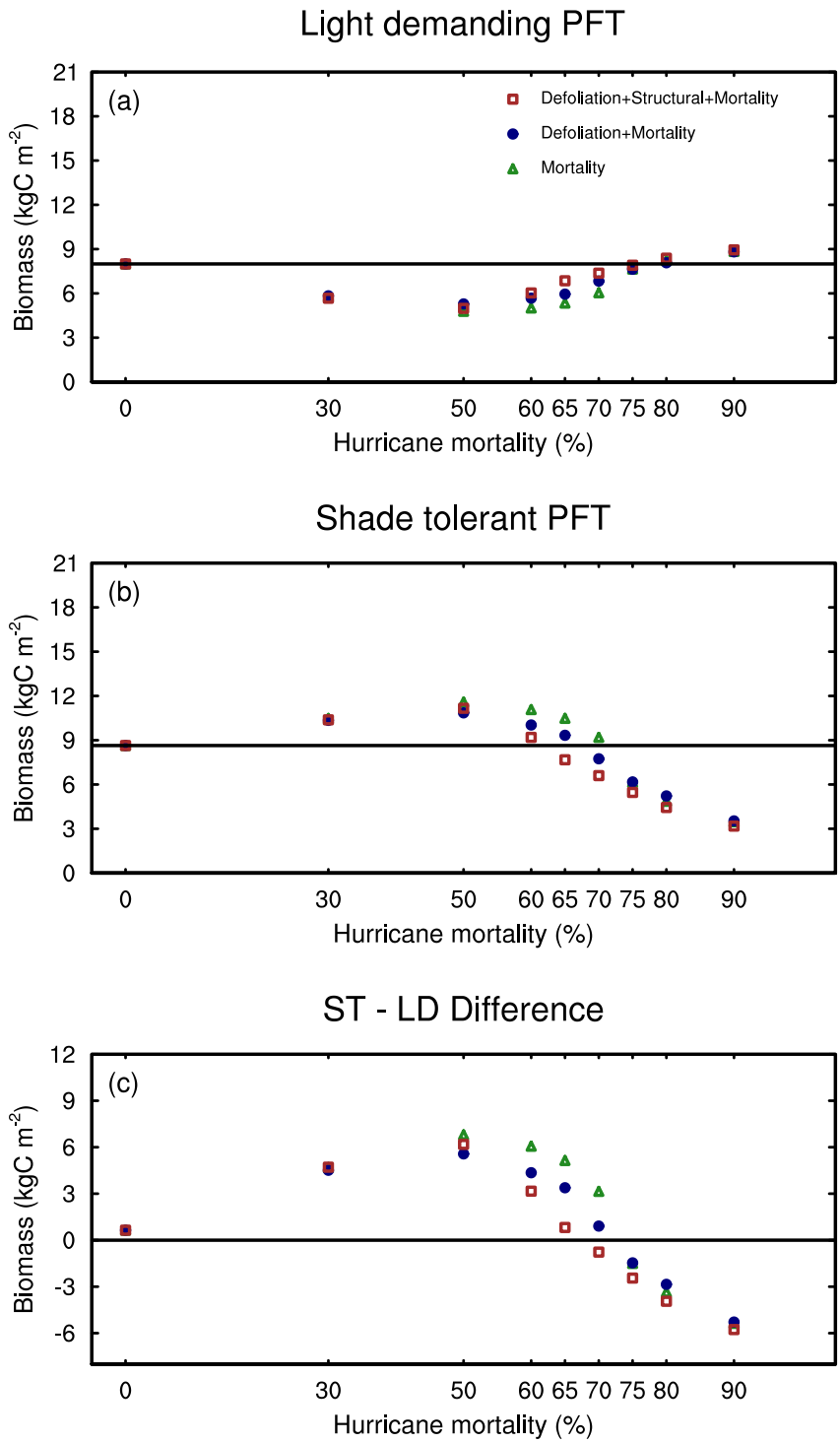

Figure 2. The mean biomass in the last 10 years (2008–2017) of the three simulation groups in Table S2 in Supporting Information S1. The green triangles indicate the mortality-only simulations (Experiment A1), the navy circles indicate the defoliation and mortality simulations (Experiment A2), and the brown squares indicate the defoliation, structural biomass reduction and mortality (Experiment A3) simulations.

damage (i.e., hurricane mortality rates larger than 75%), other types of forest damage (defoliation and structural biomass reduction) could only have limited effects on characterizing the PFT biomass divergency in terms of its recovery (Table S2 in Supporting Information S1 and Figure 2c). These simulations are based on a hypothetical

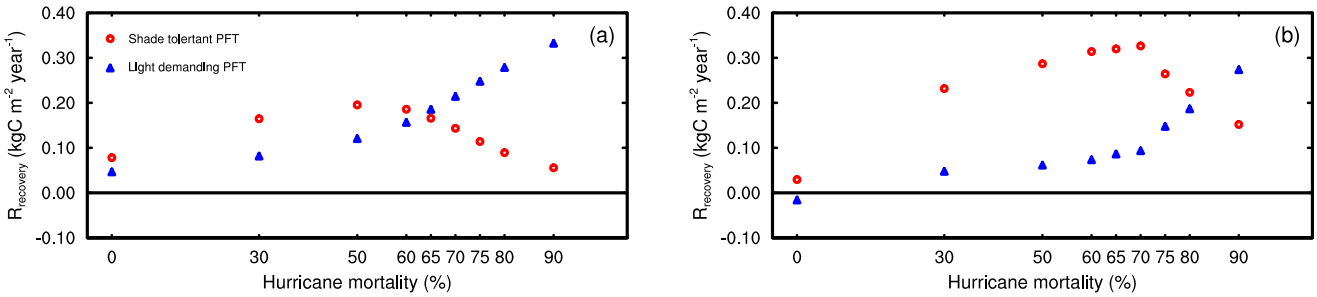

Figure 3. The linear regression coefficient of biomass recovery ($R_{recovery}$) over time (1951–1960) for experiments with D-$SB_{reduction}$ and varied hurricane mortality rates. (a) shows the $R_{recovery}$ values obtained by using the restart file of SPINUP1 (Experiment A3), and (b) shows the $R_{recovery}$ values obtained by using the restart file of SPINUP2 (Experiment B3). The $R_{recovery}$ of the light demanding PFT is represented by blue triangles, while that of the shade tolerant PFT are represented by the red circles.

PFT distribution (SPINUP1; Section 2.4.4). For comparison, we include the results that are obtained by using the initial file from a more realistic PFT distribution SPINUP2 (Table S3 in Supporting Information S1).

The results of the forest recovery show that the $R_{recovery}$ of the light demanding PFT increases with the growth of the hurricane mortality rates and reaches 0.33 kgC m^{-2} y^{-1} when the forest mortality rate is 90% (Figure 3a). In contrast, the $R_{recovery}$ of the shade tolerant PFT decreases with the mortality rate increase when the mortality rates are 60% or larger (Figure 3a). Figure 2 suggests that the 2008–2017 mean biomass of the light demanding and shade tolerant PFT starts to increase and decrease, respectively, when the hurricane mortality rates are larger than 60%. The variations of $R_{recovery}$ with the mortality rates suggest higher biomass recovery rates for the light demanding PFT when hurricane mortality is larger than 60%, which can explain why the light demanding PFT is favored in terms of biomass recovery when the hurricane mortality rates are ≥60%. This result implies that the ELM-FATES simulated tropical forests at Bisley are dominated by light demanding species when the forests experience severe hurricane damage.

We also use the restart file from SPINUP2 to perform the same simulations represented in Table S2 in Supporting Information S1 and display results in Table S3 in Supporting Information S1. The simulation results based on SPINUP2 and D-$SB_{reduction}$ with varied hurricane mortality rates are also used to calculate $R_{recovery}$ (Figure 3b). Figure 3b demonstrates that the $R_{recovery}$ values of the shade tolerant PFT starts to decrease when the hurricane mortality values are equal to or larger than 70%. Here, the $R_{recovery}$ values for the hurricane mortality rates 60%, 65%, 70%, and 75% are 0.31, 0.32, 0.32, and 0.26 kgC m^{-2} y^{-1}, respectively, indicating that hurricane mortality rates higher than 60% did not induce a substantial increase of $R_{recovery}$. The comparisons between Figures 3a and 3b and between Tables S2 and S3 in Supporting Information S1 suggest that with the same hurricane disturbance intensity forests dominated by shade tolerant species tend to be more resistant to severe hurricane disturbance. This conclusion is demonstrated by the relatively higher recovery rates and higher biomass values of the shade tolerant PFT in the experiments based on the model restart file of SPINUP2 (Table S3 in Supporting Information S1).

In this study, we use the recovery time frame 1951–1960 to calculate $R_{recovery}$, and we also calculate $R_{recovery}$ during different recovery time frame to justify the use of the results during 1951–1960. Figure S4 in Supporting Information S1 suggests that using a different time frame to calculate $R_{recovery}$ will not alter the conclusion; that is $R_{recovery}$ of the shade tolerant PFT decreases with the mortality rate increase when the hurricane mortality rates are 60% or larger (Figures 3a and Figure S4 in Supporting Information S1). The values of $R_{recovery}$ tend to decrease with the increase of the forest recovery time frame, and this conclusion is obtained from the comparison between Figures S4a–S4b and S4c–S4d in Supporting Information S1. Similar to the results based on SPINUP1, the $R_{recovery}$ values obtained from SPINUP2 vary with the $R_{recovery}$ calculation time frame and suggest a same conclusion that $R_{recovery}$ starts to decline when hurricane mortality values are ≥70% (Figures 3b and Figure S5 in Supporting Information S1). Therefore, altering the $R_{recovery}$ calculation time frame will not fundamentally change the research results, and we use the $R_{recovery}$ values calculated during 1951–1960 (the first 10 years after the simulated hurricane) for the $R_{recovery}$ analyses of this study.

3.2.2. Hurricane Disturbance Simulations With Observed Biomass Composition and Mortality Rates in ELM-FATES

We apply D-$SB_{reduction}$ and the above discussed three groups of hurricane mortality rates to perform the model simulations (C1, C2, and C3; Section 2.4.5; Figure 4). Here, we note that the simulation with a 100% defoliation,

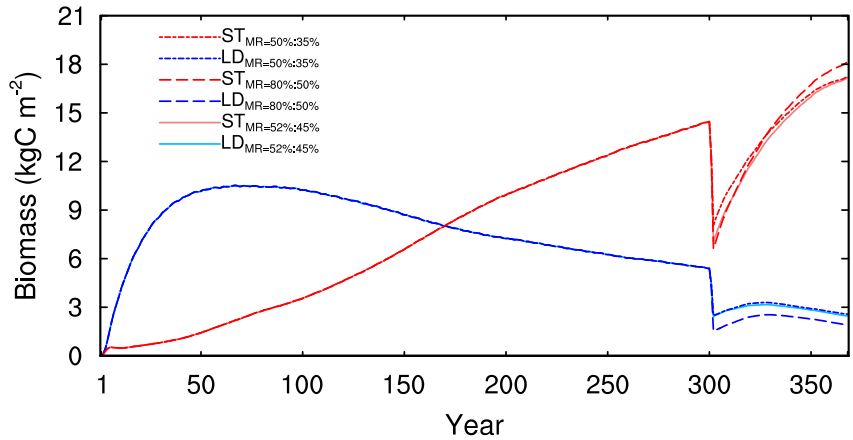

Figure 4. The forest development trajectories of SPINUP2 (1–300 years) and recovery trajectories (301–368 years) with hurricane disturbance scenarios (C1, C2, and C3; Table S4 in Supporting Information S1) included. All the simulations have defoliation and structural biomass reduction implemented. MR represents mortality rate. The light-blue and light-coral colors are representing hurricane mortality rates of 52% and 45% for the light-demanding (LD) and shade tolerant (ST) PFTs, respectively. The dashed lines represent hurricane mortality rates of 80% and 50% for the LD and ST PFTs, respectively. The dot-dashed lines represent hurricane mortality rates of 50% and 35% for the LD and ST PFTs, respectively.

20% sapwood and structural organ biomass reduction, and observational-based mortality rates can induce a ~50% AGB reduction. Specifically, the pre-Hugo AGB is 15.4 kgC m^{-2}, and the post-Hugo AGB is 7.3 kgC m^{-2}. Figure 4 shows the total forest biomass changes of the two PFTs, which have a similar reduction rate of AGB. This result is consistent with the AGB reduction discussed by Drew et al. (2009) and indicates a reasonable experimental design in terms of representing hurricane-Hugo induced forest damage. Table S4 in Supporting Information S1 summarizes the model simulated $R_{recovery}$, which is obtained from linear regression coefficient of the total biomass during 1951–1960. These three groups of simulations show the same $R_{recovery}$ of the light demanding PFT, while $R_{recovery}$ increases with the mortality rates for the shade tolerant PFT. The $R_{recovery}$ comparison between C1–3 suggests that C2 has the highest $R_{recovery}$ value of the shade tolerant PFT because of the highest hurricane mortality rates of the two PFTs (Table S4 in Supporting Information S1 and Figure 4). This change could be associated with the high hurricane mortality rates (80%) of the light demanding PFT, which only has 27% of the total biomass of the two PFTs before the hurricane disturbance. The shade tolerant PFT is then favored because of the relatively high pre-hurricane biomass ratio (73%) and relatively low hurricane mortality rates compared to those of the light demanding PFT. More detailed analyses are included in Text S2 in Supporting Information S1. We conclude that under SPINUP2 conditions, the shade tolerant PFT dominates the canopy to start and retains its dominant position.

Table 3
The Random Forest Importance Quantification of the Difference of Key Parameters and Hurricane Mortality Rates Between the Two PFTs For the Post-Hurricane Forest Recovery During 1951–1960 Following the Hurricane Disturbance Happened on 1 September 1950 (Experiment D)

Factor names	Meaning	$R_{LD} \geq R_{ST}$	$R_{LD} < R_{ST}$
Mor_diff	Hurricane mortality difference	0.148	0.284
Bmort_diff	Background mortality difference	0.146	0.117
Slatop_diff	Specific leaf area difference	0.138	0.099
Leaf_long_diff	Leaf longevity difference	0.137	0.118
Vcmax_diff	$Vcmax_{25,top}$ difference	0.133	0.104
Wood_den_diff	Wood density difference	0.104	0.093
Root_long_diff	Root longevity difference	0.098	0.083
Leafnc_diff	Leaf N:C ratio difference	0.096	0.103

Note. There were 236 ensemble cases with $R_{LD} \geq R_{ST}$ and 1864 cases with $R_{LD} < R_{ST}$.

3.3. Parameter Sensitivity Tests in ELM-FATES

We conduct a feature analysis using RF models for the response variables $R_{recovery}$ and the biomass partitions at the end of the experiment (averaged biomass by PFTs during 2008–2017; Experiment D in Table 2). For $R_{recovery}$ with both $R_{LD} \geq R_{ST}$ and $R_{LD} < R_{ST}$, the hurricane mortality difference (mor_diff) and the background mortality difference (bmort_diff) are the two primary factors influencing $R_{recovery}$. The parameter difference of specific leaf area (slatop_diff) is the third most important factor for $R_{LD} \geq R_{ST}$, while the parameter difference of leaf longevity (leaf_long_diff) is equally important to bmort_diff for $R_{LD} < R_{ST}$ (Table 3). For the rest of the features, their importance is similar, particularly for the simulations with $R_{LD} < R_{ST}$, suggesting complicated interactions among different plant traits in terms of governing the biomass recovery rates. Overall, $R_{recovery}$ status is primarily regulated by mor_diff. The divergency of some plant traits is also essential to the post-hurricane $R_{recovery}$ status, and these plant traits include background mortality, specific leaf area, and leaf longevity.

Table 4
The Random Forest Importance Quantification of the Difference of Key Parameters and Hurricane Mortality Values Between the Two PFTs For the Forest Recovery in the Last 10 Years of a 68-Year Model Simulation, Where a Hurricane Disturbance Happened on September 1st of 1950 (Experiment D)

Factor names	Meaning	LD ≥ 29%	ST ≥ 71%
Mor_diff	Hurricane mortality difference	0.302	0.142
Bmort_diff	Background mortality difference	0.148	0.120
Vcmax_diff	$Vcmax_{25,top}$ difference	0.113	0.108
Slatop_diff	Specific leaf area difference	0.101	0.108
Root_long_diff	Root longevity difference	0.090	0.111
Leafnc_diff	Leaf N:C ratio difference	0.088	0.137
Wood_den_diff	Wood density difference	0.080	0.141
Leaf_long_diff	Leaf longevity difference	0.078	0.134

Note. There were 35 ensemble cases with LD ≥ 29% and 1765 cases with ST>71%.

Similar to the feature importance analysis of $R_{recovery}$, we study the factors that determine the average biomass partitions during final 10 years of our experiment (2008–2017). Here, mor_diff, bmor_diff, and $Vcmax_{top,25}$ difference (vcmax_diff) are the three most important parameters contributing to LD > 29%, while the first three most important parameters for ST > 71% are mor_diff, wood density difference (wood_den_diff), and leafnc_diff (Table 4). The feature importance of each factor is discussed in Text S3 in Supporting Information S1. The discussions above suggest that mor_diff is the most essential factor in determining $R_{recovery}$ and biomass partitions during 2008–2017. Furthermore, bmort_diff and vcmax_diff are also important factors in determining LD > 29%, while wood_den_diff and leafnc_diff are crucial to ST > 71%.

To further study how parameter variations determine forest biomass recovery, we analyze the biomass recovery feature of Group 2 of Experiment D, which is based on the observed pre-Hugo biomass partition and hurricane mortality rates of the two PFTs (Figure S8 in Supporting Information S1). The ensemble mean biomass values in the last 10 simulation years are 3.15 ± 1.46 and 18.72 ± 2.88 kgC m^{-2} for the light demanding and shade tolerant PFTs, respectively, where the biomass portion of the light demanding PFT is reduced to 17%, lower than that before the hurricane (29%). The regression coefficient values of biomass development during 2008–2017 are −0.02 and 0.07 for the same two PFTs, respectively. Therefore, with parameter perturbations, the shade tolerant PFT is still the dominant vegetation type at Bisley after hurricane Hugo. Because the parameter perturbation method of different subgroups (Table S5 in Supporting Information S1) are identical and the standard deviation values of different subgroups in Table S5 in Supporting Information S1 are very similar, we did not include the biomass values of different subgroups. This finding is consistent with the RF based analyses that mortality rate difference is the primary factor determining the forest biomass recovery for a certain forest represented by ELM-FATES.

3.4. Quantify ELM-FATES Simulated Forest Status With Existing Observational Data Sets

Bisley does not have an established flux tower to provide continuous carbon and water flux measurements. Thus, we use satellite measurement based GPP and ET products (Section 2.6 and Experiment E; Table 2) to evaluate whether ELM-FATES reasonably simulates the carbon and water fluxes at Bisley under recovery from hurricane disturbance. Some of the data sets are not available until 2017, and they are FluxCom and PT-JPL (Table S6 in Supporting Information S1); thus, we use the longest possible data record for each product to calculate the seasonality. Here, the common period of the three GPP data sets is 2002–2015 while that of the ET data sets is 2003–2015 (Table S6 in Supporting Information S1).

We use the model ensemble simulations based on SPINUP2 and the hurricane mortality values of D1, which has the biomass partitions and hurricane mortality rates based on observations. We estimate the GPP and ET seasonality by using the model output during 2002–2015 and furing 2003–2015, respectively, and then calculate the ensemble mean of the 350 members with perturbations on the seven parameters of the two PFTs (Section 2.5). The seasonality of data products is also calculated.

The model-data comparison shows that the GPP products from different sources have large variability. The GPP of model ensemble mean has lower magnitude than the GPP from MODIS and OCO-2, and it has a similar magnitude to the GPP from FluxCom (Figure 5a). The annual GPP values of the ELM-FATES ensemble mean and FluxCoM are 2.6 and 2.7 kgC m^{-2} $year^{-1}$, respectively. The multi-product mean GPP (3.2 kgC m^{-2} $year^{-1}$) has higher magnitude than that of ELM-FATES. However, the correlation coefficient between the multi-product mean and model ensemble mean of GPP is 0.97, which indicates that the GPP seasonality represented by ELM-FATES is quite consistent with that represented by the mean of a variety of data products. Thus, ELM-FATES can simulate reasonable GPP seasonality but simulated annual GPP is 17% lower than the multi-data mean (Figure 5a).

We also perform a similar model-data comparison for ET. The annual mean ET from PT-JPL is 104.7 mm $month^{-1}$, while that from the model ensemble mean is 93.5 mm $month^{-1}$, suggesting similar ET magnitudes between PT-JPL and ELM-FATES. The ET from both FluxCom and MODIS show higher magnitude than the model

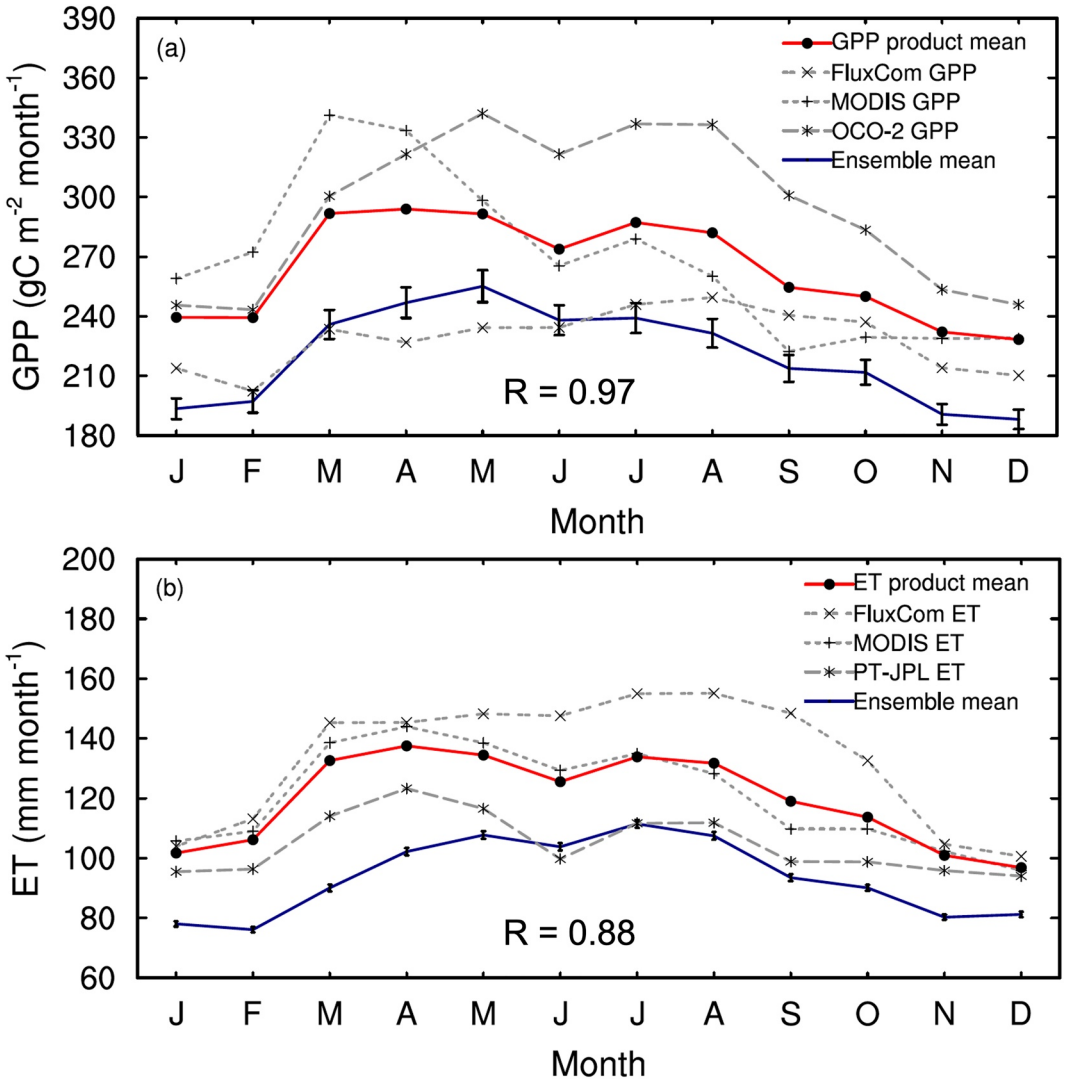

Figure 5. (a) GPP and (b) ET comparison between model ensemble simulations that use the initial condition of SPINUP2 and the hurricane mortality rates of D1 and observation-based products (Experiment E). R is the correlation coefficient between the ensemble mean of ELM-FATES (navy lines) and the mean of different data products (red lines).

ensemble mean. The multi-product mean ET on an annual basis is 119.5 mm month^{-1}, which is 26 mm month^{-1} more than that of the model ensemble mean. The correlation coefficient between the multi-product mean and model ensemble mean of ET is 0.88, which also demonstrates that the ET seasonality represented by ELM-FATES is quite consistent with that represented by the mean of a variety of data products (Figure 5b).

By using the same data sources, we also study the interannual variability of GPP and ET. The ELM-FATES simulated GPP and ET are lower than the three-product mean of each variable, similar to the seasonal-based analysis (Figure 5 and Figure S9 in Supporting Information S1). The ELM-FATES simulated GPP has a similar magnitude to FluxCom GPP, while the model simulated ET has a similar magnitude to PT-JPL-ET (Figure S9 in Supporting Information S1). Overall, ELM-FATES does a better job in reproducing seasonality than interannual variability in terms of the correlation coefficient of both GPP and ET (Figure 5 and Figure S9 in Supporting Information S1).

4. Discussion

In this study, we refine the parametrization for two PFTs in ELM-FATES to simulate forest recovery following a major hurricane in Puerto Rico. We implement defoliation, structural biomass reduction, and various hurricane mortality rates in ELM-FATES, and quantify the forest biomass recovery rates and recovery status between the

light demanding and shade tolerant PFTs by performing (a) hypothetical simulations, (b) quasi-realistic simulations, and (c) ensemble model simulations with different parameter values (Table 2). This research also uses the random forest feature importance estimates to identify model parameters and hurricane mortality rates that have larger impacts on the simulations. We analyze $R_{recovery}$ during the first decade following the simulated hurricane (1951–1960) and the forest biomass recovery status during the final decade (2008–2017) of the simulations. We focus on biomass because it integrates the effects of multiple processes (e.g., primary production, carbon allocation, and respiration), and it is well represented in empirical studies.

Following the example set by Huang et al. (2020), we explored the coexistence of two PFTs in ELM-FATES. Coexistence is challenging in FATES, and the model simulated PFT-level biomass can be sensitive to certain parameters. By using the Community Land Model with FATES implemented (i.e., CLM-FATES), Huang et al. (2020) performed 70 model ensemble simulations, and only had one parameter set (1.4%) selected with reasonable fractions of two PFTs and minor errors compared to observations. Small changes in sensitive parameters ($Vcmax_{top,25}$ and specific wood density) led to substantial differences in PFT biomass between SPINUP1 and SPINUP2. Under the SPINUP1 cases when PFTs have nearly equal biomass, when the hurricane mortality rates are ≥60%, the forests at Bisley shift composition toward the light demanding species within 50–70 years of disturbance. Due to a relatively higher portion of the pre-hurricane shade tolerant biomass, the forest represented by SPINUP2 does not have a tendency developing to a light demanding dominant system when the hurricane mortality rates are 60% for the two PFTs (Figure not shown). However, hurricanes inducing forest mortality rates 60%–70% can cause relatively highest $R_{recovery}$ values (Figure 3b). Thus, pre-hurricane forest composition explored via SPINUP1 and SPINUP2 has a strong influence on $R_{recovery}$ variations between PFTs (Figure 3).

The random forest feature importance study shows that both the hurricane mortality and the background mortality differences between the two PFTs are crucial to the PFT-level $R_{recovery}$ during the first decade (1951–1960) following the simulated hurricane and the biomass values averaged during 2008–2017. $R_{recovery}$ is also closely related to plant trait divergence determined parameter value difference of specific leaf area and of leaf longevity, while biomass composition of the two PFTs during 2008–2017 are sensitive to the parameter value difference of $Vcmax_{top,25}$, wood density, and leaf N:C. Thus, the results imply that in a forest with a certain biomass composition of different PFTs, post-hurricane forest recovery is sensitivity to both the environmental factor (i.e., hurricane mortality rates) and the plant-trait differences (e.g., background mortality, leaf longevity).

In this study, we use three GPP and three ET products to evaluate the GPP and ET simulations of ELM-FATES. With observational constrained parameters and observational based pre-Hugo biomass composition and hurricane mortality rates, ELM-FATES can reasonably represent the GPP and ET seasonality but with these two fluxes low biased compared to the multi-product mean values at Bisley.

4.1. Defoliation Representation in ELM-FATES

To implement hurricane disturbance with varied intensity in ELM-FATES, we modify the modules of phenology, structural biomass turnover, and mortality. Defoliation is the most common type of damage caused by hurricanes in Puerto Rico (Brokaw & Walker, 1991). Walker et al. (1992) estimated post-Hugo defoliation at Bisley and El Verde by counting the number of trees that had lost two thirds of their branches with diameter values larger than 1 cm. Basnet et al. (1992) performed post-Hugo data collection at Bisley by considering defoliation as complete loss of foliage from the canopy. The defoliation includes trees that remained standing but were completely defoliated with missing twigs and minor branches. Different measurement criteria can result in very different defoliation rate values. For example, Walker et al. (1992) reported defoliation rates for most of the study species as larger than 89%, while Basnet et al. (1992) estimated defoliation rates range from 0% to 46% among the study species, including the light demanding and shade tolerant species. Given the varied data collection methods corresponding to different defoliation rates, we did not further identify the advantages or limitations of different defoliation estimates. Thus, we use the 100% defoliation rate, which results in 1.2% instantaneous total biomass reduction, and further address the post-hurricane forest recovery difference induced by using varied hurricane mortality rates.

4.2. Hurricane Induced Forest Mortality

Hurricane mortality varies among species and depends on the pre-hurricane conditions of the forests. It has been demonstrated that pioneer species with low wood density are generally more vulnerable to hurricanes than old-growth high wood density species (Canham et al., 2010; Zimmerman et al., 1994). For example,

Zhang, Bra, et al. (2022) and Zhang, Heartsill-Scalley, and Bras (2022) suggest that the early successional PFT, which are defined more inclusively as the light demanding PFT in this study, have the highest mortality rates among four PFTs, early , mid-, and late-successional and palm. Furthermore, pre-hurricane soil moisture condition is a major controlling factor of hurricane induced forest damage (Xi et al., 2008). For example, stem breakage is the dominant type of damage in dry soils, while uprooting is more common in wet soils (Xi et al., 2008). Therefore, the hurricane intensity, and the pre-hurricane forest status and forest environmental conditions are essential factors closely related to hurricane damage intensity. We acknowledge the complexity of forest responses to hurricane disturbance (Bomfim et al., 2022; Uriarte et al., 2019). In this study, we did not prescribe the pre-hurricane soil moisture condition in ELM-FATES, because the model is not able to represent the impacts of pre-hurricane soil moisture condition on forest damage severity due to hurricane. Thus, the main scope of this research is to quantify the sensitivity of post-hurricane forest recovery to the hurricane mortality rates, with consideration of the importance of other essential parameters characterizing the two PFTs.

In this study, the ELM-FATES simulations suggest a tendency of the tropical forests at Bisley to shift toward the light demanding PFT, when hurricane disturbance is severe with hurricane mortality >60% for both the light demanding and shade tolerant PFTs with a variety of biomass compositions, from a nearly equal partition between these two PFTs to a shade tolerant dominant (i.e., ~70%) composition. It is likely that hurricane intensity will increase over the coming decades (Emanuel, 2005; Knutson et al., 2019; Walsh et al., 2016). Furthermore, climate models also predict enhanced hurricane activity in the tropical Atlantic. This enhancement is associated with weakened vertical wind shear in the Main Development Region, which can favor more hurricane activity in the tropical North Atlantic (Ting et al., 2019). In a future with more severe hurricanes (e.g., Hurricane Hugo, a category 4 hurricane), we expect forest compositional shifts, with a tendency for more palms because of the low palm mortality in hurricanes compared to other tree species (Uriarte et al., 2019; Zhang, Bra, et al., 2022; Zhang, Heartsill-Scalley, & Bras, 2022).

4.3. Crown Damage Module

We acknowledge that the representation of hurricane disturbance is still limited in ELM-FATES. Thus, we perform hypothetical simulations to study the sensitivity of forest recovery to hurricane disturbance with varied intensity and to the key model parameters representing plant traits of different PFTs. To advance future studies of hurricane disturbance and recovery, we will use ELM-FATES with new model features implemented. For example, a crown damage module is implemented into ELM-FATES (Needham et al., 2022). Specifically, the crown damage reduces AGB, changes forest structure, increases carbon starvation mortality, reduces growth rates, and changes competitive dynamics between PFTs (Needham et al., 2022). As the next step, we will perform a more detailed model-data comparison study by using in situ DBH, tree height, and litterfall measurements, and the crown damage module.

4.4. ELM-FATES Simulated Hurricane Impacts on Puerto Rican Forest Recovery

Northeastern Puerto Rico is impacted more than elsewhere in Puerto Rico, due to the typical east-to-west Atlantic hurricane moving direction (Boose et al., 2004). Since 1989, nine hurricanes (including Hugo) have affected Bisley. We simulated a single hurricane disturbance. Because multiple disturbances are possible, we intend to use ELM-FATES to explore the effect of more frequent intense disturbances. The research results imply that when a canopy is dominated by the shade tolerant PFT, the recovery of the shade tolerant PFT will suppress the succession of light demanding PFT. For example, in Experiment A, when hurricane mortality rates equal 50%, $R_{recovery}$ of the shade tolerant PFT is 0.2 kgC m^{-2} $year^{-1}$ for a nearly even initial biomass partition between the light demanding and shade tolerant PFT (Figure 3a) but 0.3 kgC m^{-2} $year^{-1}$ when the shade tolerant PFT dominates (Figure 3b). This comparison indicates that in the simulation with SPINUP2, the pre-hurricane dominance and rapid recovery of the shade tolerant canopy limits regrowth for the light demanding PFT. Only when the hurricane induced damage is severe enough to generate sufficient open canopy areas, the $R_{recovery}$ values of the light demanding PFT can be larger than that of the shade tolerant PFT (Figure 3b). The RF feature importance analyses also suggest that the hurricane mortality rate difference between PFTs may effectively suppress the recovery of the light demanding PFT, highlighting the importance of using the observed mortality rates to constrain model simulations of post-hurricane recovery.

4.5. Using the Global Data Sets to Benchmark ELM-FATES at Bisley

Because Bisley does not have established flux towers, we use different global data products to benchmark ELM-FATES at the monthly time scale; all the data sets have different spatial resolutions (Table S5 in Supporting Information S1). The comparison shows limited consistency between data sets (Figure 5), implying large uncertainties (Anav et al., 2015; Sriwongsitanon et al., 2020; Zhang & Ye, 2022). Rather than perform product comparison and generating weighted GPP (e.g., Zhang & Ye, 2022) and ET products, we use the arithmetic mean of different data products. We show that the GPP and ET seasonality of ELM-FATES is in good agreement with that represented by the data products. This result indicates that with the constrained parameterization and reasonable model physics, ELM-FATES can be used to represent the photosynthetic carbon assimilation and land-to-atmosphere water exchange at our study site. Here, ELM-FATES simulated ET has a similar magnitude to the PT-JPL ET product but lower than the arithmetic mean of the three ET products (Figure 5b), which suggest a mean annual ET 119.5 mm month^{-1} (i.e., 4 mm day^{-1}). As suggested by eddy covariance measurement-based studies (Miller et al., 2011; Rocha et al., 2004), the mean annual ET of tropical forests is usually less than 4 mm day^{-1} (i.e., ∼3.5 mm day^{-1}), which implies the uncertainty and high bias of the data products (Table S5 in Supporting Information S1; Figure 5b). In this study, the model-data comparison period starts from 2002 to 2003 for GPP and ET, respectively, since which most of the products are available; while the time span between 1989 and 2002 is 13 years. Here, we did not try to match the model-data comparison time period, since both GPP and ET are ecosystem fluxes, which usually have quicker response and recovery time frame than carbon stocks (e.g., total ecosystem carbon). In other words, the comparison time frame of ecosystem fluxes is less concerned than that of biomass.

5. Conclusion

ELM-FATES can represent the hurricane disturbance and recovery of the tropical wet forests of Puerto Rico. Model parameterization is essential to the co-existence of the light demanding and shade tolerant PFTs. Simulations with the same mortality rates for the two PFTs show that the light demanding PFT is favored by severe hurricane disturbance with the hurricane mortality value larger than 60%, and this estimated mortality value increases with the biomass portion growth of the shade tolerant PFT. With mortality rates closer to those observed in the field for light demanding and shade tolerant species, the shade tolerant PFT dominates forest recovery rates. Based on the Random Forests feature importance estimates, hurricane mortality and background mortality are the two key factors regulating the post-hurricane forest recovery rates and forest biomass composition. The research findings of this study imply species shifts in the Puerto Rico tropical forest as a result of climate change induced hurricane frequency and intensity increase. To better interpret these changes, some key processes (e.g., wind damage on forests) and more plant traits (e.g., palms) are suggested to be implemented in DGVMs. With enhanced model capacity and advanced model exploration, which includes thoroughly comparison between the model and inventory data, the understanding on the dynamics of Puerto Rico tropical forests could be profoundly improved.

Conflict of Interest

The authors declare no conflicts of interest relevant to this study.

Data Availability Statement

The ELM-FATES source code, related surface and domain data files, and the scripts used to develop the figures of this study are available at https://zenodo.org/records/10058828. The Daymet meteorological fields (Kao et al., 2022) are available at https://daymet.ornl.gov/. The OCO-2 SIF derived GPP (Li & Xiao, 2019) is at http://globalecology.unh.edu/data/GOSIF-GPP.html. The FluxCom data products (Jung et al., 2020) are at https://www.bgc-jena.mpg.de/geodb/projects/Home.php. MODIS data products (Mu et al., 2011; Zhao et al., 2005) are at https://modis.gsfc.nasa.gov/data/. The PT-JPL ET data are developed by Purdy et al. (2018), DOI: https://doi.org/10.1016/j.rse.2018.09.023.

Acknowledgments
We thank Adam J. Purdy for providing the PT-JPL data. We also acknowledge Dr. Xiaojuan Yang and Dr. Xinyuan Wei for providing insights on the ELM-FATES parameterization. This research was conducted at Pacific Northwest National Laboratory, operated for the U.S. Department of Energy by Battelle Memorial Institute under contract DE-AC05-76RL01830. This study was supported by the Department of Energy's (DOE) Office of Biological and Environmental Research as part of the Terrestrial Ecosystem Science program through the Next-Generation Ecosystem Experiments (NGEE)-Tropics project. *Financial support*. This research was supported by the U.S. Department of Energy, Office of Science (Grant 71073).

References

Adame, P., Brandeis, T., & Uriarte, M. (2014). Diameter growth performance of tree functional groups in Puerto Rican secondary tropical forests. *Instituto Nacional de Investigación y Tecnología Agraria y Alimentaria*, *23*(1), 52–63. https://doi.org/10.5424/fs/2014231-03644

Anav, A., Friedlingstein, P., Beer, C., Ciais, P., Harper, A., Jones, C., et al. (2015). Spatiotemporal patterns of terrestrial gross primary production: A review. *Reviews of Geophysics*, *53*(3), 785–818. https://doi.org/10.1002/2015rg000483

Antoniadis, A., Lambert-Lacroix, S., & Poggi, J. M. (2021). Random forests for global sensitivity analysis: A selective review. *Reliability Engineering and System Safety*, *206*, 107312. https://doi.org/10.1016/j.ress.2020.107312

Basnet, K., Likens, G. E., Scatena, F. N., & Lugo, A. E. (1992). Hurricane Hugo: Damage to a tropical rain forest in Puerto Rico. *Journal of Tropical Ecology*, *8*(1), 47–55. https://doi.org/10.1017/s0266467400006076

Belgiu, M., & Drăguţ, L. (2016). Random forest in remote sensing: A review of applications and future directions. *ISPRS Journal of Photogrammetry and Remote Sensing*, *114*, 24–31. https://doi.org/10.1016/j.isprsjprs.2016.01.011

Bomfim, B., Walker, A. P., McDowell, W. H., Zimmerman, J. K., Feng, Y., & Kueppers, L. M. (2022). Linking soil phosphorus with forest litterfall resistance and resilience to cyclone disturbance: A pantropical meta-analysis. *Global Change Biology*, *28*(15), 4633–4654. https://doi.org/10.1111/gcb.16223

Boose, E. R., Serrano, M. I., & Foster, D. R. (2004). Landscape and regional impacts of hurricanes in Puerto Rico. *Ecological Monographs*, *74*(2), 335–352. https://doi.org/10.1890/02-4057

Breiman, L. (2021). Random forests. *Machine Learning*, *45*(1), 5–32. https://doi.org/10.1023/a:1010933404324

Brokaw, N., Zimmerman, J. K., Wilig, M. R., Camilo, G. R., Covich, A. R., Crowl, T. A., et al. (2012). Response to disturbance. Pages 201–271. In N. Brokaw, T. A. Crowl, A. E. Lugo, W. H. McDowell, F. N. Scatena, R. B. Waide, et al. (Eds.), *A Caribbean Forest Tapestry: The multidimensional nature of disturbance and response*. Oxford University Press.

Brokaw, V. L., & Walker, L. R. (1991). Summary of the effects of Caribbean hurricanes on vegetation. *Biotropica*, *23*(4), 442–447. https://doi.org/10.2307/2388264

Brown, S., Lugo, A. E., Silander, S., & Liegel, L. (1983). *Research history and opportunities in the Luquillo experimental forest, gen* (p. 128) Tech, Rep. SO-44. US Department of Agriculture, Forest Service, Southern Forest Experiment Station.

Burrows, S. M., Maltrud, M., Yang, X., Zhu, Q., Jeffery, N., Shi, X., et al. (2020). The DOE E3SM v1.1 biogeochemistry configuration: Description and simulated ecosystem-climate responses to historical changes in forcing. *Journal of Advances in Modelling Earth Systems*, *12*(9), e2019MS001766. https://doi.org/10.1029/2019ms001766

Canham, C. D., Thompson, J., Zimmerman, J. K., & Uriarte, M. (2010). Variation in susceptibility to hurricane damage as a function of storm intensity in Puerto Rican tree species. *Biotropica*, *42*(1), 87–94. https://doi.org/10.1111/j.1744-7429.2009.00545.x

Chazdon, R. L. (2003). Tropical forest recovery: Legacies of human impact and natural disturbances. Perspectives in Plant Ecology. *Evolution and Systematics*, *6*(1–2), 51–71. https://doi.org/10.1078/1433-8319-00042

Chen, Y. Y., Gardiner, B., Pasztor, F., Blennow, K., Ryder, J., Valade, A., et al. (2018). Simulating damage for wind storms in the land surface model ORCHIDEE-CAN (revision 4262). *Geoscientific Model Development*, *11*(2), 771–791. https://doi.org/10.5194/gmd-11-771-2018

Da Rocha, H. R., Goulden, M. L., Miller, S. D., Menton, M. C., Pinto, L. D., de Freitas, H. C., & e Silva Figueira, A. M. (2004). Seasonality of water and heat fluxes over a tropical forest in eastern Amazonia. *Ecological Applications*, *14*(sp4), 22–32. https://doi.org/10.1890/02-6001

Dirmeyer, P. A., Huang, K., Lydeen, N., Manthos, Z. H., Knapp, S., & Hay-Chapman, F. M. (2021). Projected hydroclimate changes driven by carbon dioxide trends and vegetation modeling in CMIP6. *Earth's Future*. https://doi.org/10.1002/essoar.10506162.1

Drew, A. P., Boley, J. D., Zhao, Y., Johnston, M. H., & Wadsworth, F. H. (2009). Sixty-two years of change in subtropical wet forest structure and composition at El Verde, Puerto Rico. *Interciencia*, *34*, 34–40.

Emanuel, K. (2005). Increasing destructiveness of tropical cyclones over the past 30 years. *Nature*, *436*(7051), 686–688. https://doi.org/10.1038/nature03906

Eyring, V., Gleckler, P. J., Heinze, C., Stouffer, R. J., Taylor, K. E., Balaji, V., et al. (2016). Towards improved and more routine Earth system model evaluation in CMIP. *Earth System Dynamics*, *7*(4), 813–830. https://doi.org/10.5194/esd-7-813-2016

Feng, X., Uriarte, M., Gonzalez, G., Reed, S., Thompson, J., Zimmerman, J. K., & Murphy, L. (2017). Improving predictions of tropical forest response to climate change through integration of field studies and ecosystem modeling. *Global Change Biology*, *24*, 1–20. https://doi.org/10.1111/gcb.13863

Fisher, R. A., McDowell, N., Purves, D., Moorcroft, P., Sitch, S., Cox, P., et al. (2010). Assessing uncertainties in a second-generation dynamic vegetation model caused by ecological scale limitations. *New Phytologist*, *187*(3), 666–681. https://doi.org/10.1111/j.1469-8137.2010.03340.x

Fisher, R. A., Muszala, S., Verteinstein, M., Lawrence, P., Xu, C., McDowell, N. G., et al. (2015). Taking off the training wheels: The properties of a dynamic vegetation model without climate envelopes, CLM4.5(ED). *Geoscientific Model Development*, *8*(11), 3593–3619. https://doi.org/10.5194/gmd-8-3593-2015

Garcia-Martino, A. R., Warner, G.S., Scatena, F. N., & Civco, D. L. (1996). Rainfall, runoff and elevation relationships in the Luquillo Mountins of Puerto Rico. *Caribbean Journal of Science*, *32*, 413–424.

Hao, D., Bisht, G., Gu, Y., Lee, W. L., Liou, K. N., & Leung, L. R. (2021). A parameterization of sub-grid topographical effects on solar radiation in the E3SM land model (version 1.0): Implementation and evaluation over the Tibetan Plateau. *Geoscientific Model Development*, *14*(10), 6273–6289. https://doi.org/10.5194/gmd-14-6273-2021

Heartsill-Scalley, T., Scatena, F. N., Lugo, A. E., Moya, S., & Estrada, C. R. (2010). Changes in structure, composition, and nutrients during 15 years of hurricane-induced succession in a subtropical wet forest in Puerto Rico. *Biotropica*, *42*(4), 455–463. https://doi.org/10.1111/j.1744-7429.2009.00609.x

Heartsill-Scalley, T. H. (2017). Insights on forest structure and composition from long-term research in the Luquillo Mountains. *Forest*, *8*(6), 204. https://doi.org/10.3390/f8060204

Holm, J. A., Knox, R., Zhu, Q., Fisher, R. A., Koven, C. D., Nogueira Lima, A. J., et al. (2020). The central Amazon biomass sink under current and future atmospheric CO_2: Predictions from big-leaf and demographic vegetation models. *Journal of Geophysical Research: Biogeosciences*, *125*(3), e2019JG005500. https://doi.org/10.1029/2019jg005500

Huang, B. F., & Boutros, P. C. (2016). The parameter sensitivity of random forests. *BMC Bioinformatics*, *17*(1), 1–13. https://doi.org/10.1186/s12859-016-1228-x

Huang, M., Xu, Y., Longo, M., Kellerer, M. M., Knox, R., Koven, C., & Fisher, R. (2020). Assessing impacts of selective logging on water, energy, and carbon budgets and ecosystems dynamics in Amazon forests using the functionally assembled terrestrial ecosystem simulator. *Biogeosciences*, *17*(20), 4999–5023. https://doi.org/10.5194/bg-17-4999-2020

Jung, M., Schwalm, C., Migliavacca, M., Walther, S., Camps-Valls, G., Koirala, S., et al. (2020). Scaling carbon fluxes from eddy covariance sites to globe: Synthesis and evaluation of the FLUXCOM approach [Dataset]. Biogeosciences, *17*(5), 1343–1365. https://doi.org/10.5194/bg-17-1343-2020

Kao, S.-C., Thornton, P. E., Thornton, M. M., Shrestha, R., & Walker, A. P. (2022). Sub-daily climate forcings for Puerto Rico [Dataset]. ORNL DAAC. https://doi.org/10.3334/ORNLDAAC/1977

Kattge, J., Diaz, S., Lavorel, S., Prentice, I. C., Leadley, P., Bönisch, G., et al. (2011). TRY–a global database of plant traits. *Global Change Biology*, *17*(9), 2905–2935.

Kattge, J., Knorr, W., Raddatz, T., & Wirth, C. (2009). Quantifying photosynthetic capacity and its relationship to leaf nitrogen content for global-scale terrestrial biosphere models. *Global Change Biology*, *15*(4), 976–991. https://doi.org/10.1111/j.1365-2486.2008.01744.x

Knutson, T., Landsea, C., & Emanuel, K. (2019). Tropical cyclones and climate change: A review. In *Global perspectives on tropical cyclones: From science to mitigation* (Vol. 2010, pp. 243–284).

Koven, C. D., Knox, R., Fisher, R. A., Chambers, J. Q., Christoffersen, B. O., Davies, S. J., et al. (2020). Benchmarking and parameter sensitivity of physiological and vegetation dynamics using the functionally assembled terrestrial ecosystem simulator (FATES) at Barro Colorado Island, Panama. *Biogeosciences*, *17*(11), 3017–3044. https://doi.org/10.5194/bg-17-3017-2020

Li, X., & Xiao, J. (2019). A global, 0.05-degree product of solar-induced chlorophyll fluorescence derived from OCO-2, MODIS, and reanalysis data [Dataset]. Remote Sensing, *11*(5), 517. https://doi.org/10.3390/rs11050517

Mesinger, F., DiMegoand, G., Kalnay, E., Mitchell, K., Shafran, P. C., Ebisuzaki, W., et al. (2006). North American regional reanalysis. *Bulletin America Meteorology Social*, *87*(3), 343–360. https://doi.org/10.1175/bams-87-3-343

Miller, S. D., Goulden, M. L., Hutyra, L. R., Keller, M., Saleska, S. R., Wofsy, S. C., et al. (2011). Reduced impact logging minimally alters tropical rainforest carbon and energy exchange. *Proceedings of the National Academy of Sciences of the United States of America*, *108*(48), 19431–19435. https://doi.org/10.1073/pnas.1105068108

Moorcroft, P. R., Hurtt, G. C., & Pacala, S. W. (2001). A method for scaling vegetation dynamics: The ecosystem demography model (ED). *Ecological Monographs*, *71*(4), 557–585. https://doi.org/10.1890/0012-9615(2001)071[0557:amfsvd]2.0.co;2

Mu, Q., Zhao, M., & Running, S. W. (2011). Improvements to a MODIS global terrestrial evapotranspiration algorithm [Dataset]. Remote Sensing of Environment, *115*(8), 1781–1800. https://doi.org/10.1016/j.rse.2011.02.019

Needham, J. F., Arellano, G., Davies, S. J., Fisher, R. A., Hammer, V., Knox, R., et al. (2022). Tree crown damage and its effects on forest carbon cycling in a tropical forest. *Global Change Biology*, *28*(18), 5560–5574. https://doi.org/10.1111/gcb.16318

Negron-Juarez, R. I., Holm, J. A., Faybishenko, B., Magnabosco-Marra, D., Fisher, R. A., Shuman, J. K., et al. (2020). Landsat near-infrared (NIR) band and ELM-FATES sensitivity to forest disturbances and regrowth in the Central Amazon. *Biogeosciences*, *17*(23), 6185–6205. https://doi.org/10.5194/bg-17-6185-2020

Powell, T. L., Koven, C. D., Johnson, D. J., Faybishenko, B., Fisher, R. A., Knox, R. G., et al. (2018). Variation in hydroclimate sustains tropical forest biomass and promotes functional diversity. *New Phytologist*, *219*(3), 932–946. https://doi.org/10.1111/nph.15271

Purdy, A. J., Fisher, J. B., Goulden, M. L., Colliander, A., Halverson, G., Tu, K., & Famiglietti, J. S. (2018). SMAP soil moisture improves global evapotranspiration [Dataset]. Remote Sensing of Environment, *219*, 1–14. https://doi.org/10.1016/j.rse.2018.09.023

Purves, D. W., Lichstein, J. W., Strigul, N., & Pacala, S. W. (2008). Predicting and understanding forest dynamics using a simple tractable model. *Proceedings of the National Academy of Sciences of the United States of America*, *105*(44), 17018–17022. https://doi.org/10.1073/pnas.0807754105

Reyes, G., Brown, S., Chapman, J., & Lugo, A. E. (1992). *Wood densities of tropical tree species*. General Technical Report, S0–88. United States Department of Agriculture, Forest Service.

Running, S. W., Nemani, R. R., Heinsch, F. A., Zhao, M., Reeves, M., & Hashimoto, H. (2004). A continuous satellite-derived measure of global terrestrial primary production. *BioScience*, *54*(6), 547–560. https://doi.org/10.1641/0006-3568(2004)054[0547:acsmog]2.0.co;2

Scatena, F. N., Moya, S., Estrada, C., & Chinea, J. D. (1996). The first five years in the reorganization of aboveground biomass and nutrient use following Hurricane Hugo in the Bisley Experimental Watersheds, Luquillo Experimental Forest, Puerto Rico. *Biotropica*, *28*(4), 424–440. https://doi.org/10.2307/2389086

Silver, W. L., & Miya, R. K. (2001). Global patterns in root decomposition: Comparisons of climate and litter quality effects. *Oecologia*, *129*(3), 407–419. https://doi.org/10.1007/s004420100740

Sriwongsitanon, N., Suwawong, T., Thianpopirug, S., Williams, J., Jia, L., & Bastiaanssen, W. (2020). Validation of seven global remotely sensed ET products across Thailand using water balance measurements and land use classifications. *Journal of Hydrology: Regional Studies*, *30*, 100709. https://doi.org/10.1016/j.ejrh.2020.100709

Taccoen, A., Piedallu, C., Seynave, I., Perez, V., Gégout-Petit, A., Nageleisen, L. M., et al. (2019). Background mortality drivers of European tree species: Climate change matters. *Proceedings of the Royal Society B*, *286*(1900), 20190386. https://doi.org/10.1098/rspb.2019.0386

Thessen, A. (2016). Adoption of machine learning techniques in ecology and Earth science. *One Ecosystem*, *1*, e8621. https://doi.org/10.3897/oneeco.1.e8621

Thornton, P. E., Shrestha, R., Thornton, M., Kao, S. C., Wei, Y., & Wilson, B. E. (2021). Gridded daily weather data for North America with comprehensive uncertainty quantification. *Scientific Data*, *8*(1), 190. https://doi.org/10.1038/s41597-021-00973-0

Ting, M., Kossin, J. P., Camargo, S. J., & Li, C. (2019). Past and future hurricane intensity change along the US East Coast. *Scientific Reports*, *9*(1), 1–8. https://doi.org/10.1038/s41598-019-44252-w

Tyralis, H., Papacharalampous, G., & Langousis, A. (2019). A brief review of random forests for water scientists and practitioners and their recent history in water resources. *Water*, *11*(5), 910. https://doi.org/10.3390/w11050910

Uriarte, M., Thompson, J., & Zimmerman, J. K. (2019). Hurricane Maria tripled stem breaks and doubled tree mortality relative to other major storm. *Nature Communications*, *10*(1), 1362. https://doi.org/10.1038/s41467-019-09319-2

Walker, A. P., Beckerman, A. P., Gu, L., Kattge, J., Cernusak, L. A., Domingues, T. F., et al. (2014). The relationship of leaf photosynthetic traits–Vcmax and Jmax–to leaf nitrogen, leaf phosphorus, and specific leaf area: A meta-analysis and modeling study. *Ecology and Evolution*, *4*(16), 3218–3235. https://doi.org/10.1002/ece3.1173

Walker, L. R., Voltzow, J., Ackerman, J. D., Fernaindez, D. S., & Fetcher, N. (1992). Immediate impact of Hurricane Hugo on a Puerto Rican rain forest. *Ecology*, *73*(2), 691–694. https://doi.org/10.2307/1940775

Walker, L. R. (2012). *The biology of disturbed habitats*. Oxford University Press.

Walsh, K. J., McBride, J. L., Klotzbach, P. J., Balachandran, S., Camargo, S. J., Holland, G., et al. (2016). Tropical cyclones and climate change. *Wiley Interdisciplinary Reviews: Climate Change*, *7*(1), 65–89. https://doi.org/10.1002/wcc.371

Wu, L., Kato, T., Sato, H., Hirano, T., & Yazaki, T. (2019). Sensitivity analysis of the typhoon disturbance effect on forest dynamics and carbon balance in the future in a cool-temperate forest in northern Japan by using SEIB-DGVM. *Forest Ecology and Management*, *451*, 117529. https://doi.org/10.1016/j.foreco.2019.117529

Xi, W., Peet, R. K., Decoster, J. K., & Urban, D. L. (2008). Tree damage risk factors associated with large, infrequent wind disturbances of Carolina forests. *Forestry*, *81*(3), 317–334. https://doi.org/10.1093/forestry/cpn020

Yoshimura, K., & Kanamitsu, M. (2013). Incremental correction for the dynamical downscaling of ensemble mean atmospheric fields. *Monthly Weather Review*, *141*(9), 3087–3101. https://doi.org/10.1175/mwr-d-12-00271.1

Zhang, J., Bras, R. L., Longo, M., & Heartsill-Scalley, T. (2022). The impact of hurricane disturbances on a tropical forest: Implementing a palm plant functional type and hurricane disturbance module in ED2-HuDi V1. 0. *Geoscientific Model Development*, *15*(13), 5107–5126. https://doi.org/10.5194/gmd-15-5107-2022

Zhang, J., Heartsill-Scalley, T., & Bras, R. L. (2022). *Tree census at bisley experimental watersheds since hurricane Hugo in 1989 to 2014*. Forest Service Research Data Archive.

Zhang, Y., & Ye, A. (2022). Improving global gross primary productivity estimation by fusing multi-source data products. *Heliyon*, *8*(3), e09153. https://doi.org/10.1016/j.heliyon.2022.e09153

Zhao, M., Heinsch, F. A., Nemani, R. R., & Running, S. W. (2005). Improvements of the MODIS terrestrial gross and net primary production global data set [Dataset]. Remote Sensing of Environment, *95*(2), 164–176. https://doi.org/10.1016/j.rse.2004.12.011

Zimmerman, J. K., Everham, E. M., III, Waide, R. B., Lodge, D. J., Taylor, C. M., & Brokaw, N. (1994). Responses of tree species to hurricane winds in subtropical wet forest in Puerto Rico: Implications for tropical tree life histories. *Journal of Ecology*, *82*(4), 911–922. https://doi.org/10.2307/2261454

Zimmerman, J. K., Wood, T. E., González, G., Ramirez, A., Silver, W. L., Uriarte, M., et al. (2021). Disturbance and resilience in the Luquillo experimental forest. *Biological Conservation*, *253*, 108891. https://doi.org/10.1016/j.biocon.2020.108891

References From the Supporting Information

Chave, J., Réjou-Méchain, M., Búrquez, A., Chidumayo, E., Colgan, M. S., Delitti, W. B. C., et al. (2014). Improved allometric models to estimate the aboveground biomass of tropical trees. *Global Change Biology*, *20*(10), 3177–3190. https://doi.org/10.1111/gcb.12629

Martínez Cano, I., Muller-Landau, H. C., Wright, S. J., Bohlman, S. A., & Pacala, S. W. (2019). Tropical tree height and crown allometries for the Barro Colorado Nature Monument, Panama: A comparison of alternative hierarchical models incorporating interspecific variation in relation to life history traits. *Biogeosciences*, *16*(4), 847–862. https://doi.org/10.5194/bg-16-847-2019